Current Research in Food Science 6 (2023) 100519

Contents lists available at ScienceDirect

Current Research in Food Science

journal homepage: www.sciencedirect.com/journal/current-research-in-food-science

Phenolic profile, antioxidation and anti-proliferation activity of phenolic-rich extracts from *Sanghuangporus vaninii*

Hong Gao [a,b], Chaomin Yin [a,*], Chen Li [a], Yuhong Li [a], Defang Shi [a], Xiuzhi Fan [a], Fen Yao [a], Wenjing Wu [a], Jiangtao Li [c]

[a] National Research and Development Center for Edible Fungi Processing (Wuhan), Key Laboratory of Agro-Products Cold Chain Logistics of Ministry of Agriculture and Rural Affairs, Institute of Agro-Products Processing and Nuclear-Agricultural Technology, Hubei Academy of Agricultural Sciences, Wuhan, 430064, China
[b] Research Center of Under-forest Economy in Hubei Province, Wuhan, 430064, China
[c] College of Food Science and Engineering, Central South University of Forestry and Technology, Changsha, 410004, China

ARTICLE INFO

Handling Editor: Professor A.G. Marangoni

Keywords:
Sanghuangporus vaninii
Phenolic profile
Polyphenols
Antioxidative activity
Antiproliferative activity

ABSTRACT

In this study, phenolic-rich extracts from *Sanghuangporus vaninii* (SHE) were prepared, the phenolic profile and main phenolic compound content of SHE were studied by UPLC-Orbitrap-MS, and the antioxidant and anti-proliferation activities of SHE were evaluated. The results showed that the total polyphenol content and the total flavonoid content of SHE were 42.420 ± 0.011 mg GAE/g EW and 8.504 ± 0.205 mg RE/g EW, respectively. Moreover, 14 phenolic acids and 8 flavonoids in SHE were identified, among which, the major polyphenols were protocatechualdehyde (394.68 μg/g), protocatechuic acid (196.88 μg/g), caffeic acid (96.11 μg/g), L-phenylalanine (12.72 μg/g) and (+)-taxifolin (8.59 μg/g). SHE showed strong radical scavenging, anti-lipid peroxidation and anti-DNA damage capacity *in vitro*. SHE could effectively induce HepG2 cell apoptosis via the caspases-dependent mitochondrial apoptotic pathway and arrest the cell cycle in the G0/G1 phase. The present study suggested that *S. vaninii* could be a valuable source of natural antioxidative and antiproliferative ingredients.

1. Introduction

'Sanghuang' is one of the most important groups of medicinal macrofungi in China and has been widely used in folk medicine around East Asia (Zhou et al., 2022). The earliest record of 'Sanghuang' appears in 'Shen Nong Materia Medica', a traditional Chinese medicine book that dates back to 2000 years ago, described as 'Sang'er', which grows on *Morus* trees (Zhou et al., 2022). Since modern times, there have been many taxonomic Latin names used to represent 'Sanghuang', such as *Phellinus linteus*, *Inonotus linteus* and *Inonotus sanghuang* (Zhou et al., 2022). Some years ago, Zhou et al. (2016) established a scientific fungal genus name *Sanghuangporus* to represent 'Sanghuang' based on morphological and phylogenetic data of global samples, and this taxonomic system was widely acknowledged. Currently, 14 described species of 'Sanghuang' have been accommodated in the genus *Sanghuangporus* (Zhou et al., 2022).

Sanghuangporus vaninii (Ljub.) L.W. Zhou & Y.C. Dai. is one of the famous 'Sanghuang' because of its largest share of the 'Sanghuang' application market (Guo et al., 2021). This fungus is one of the few successful artificially cultivated *Sanghuangporus* species, with high and stable yields (Zhou et al., 2022). Historically, the general public and researchers have preferred the traditional 'Sanghuang' (*S. sanghuang*, which grows on *Morus* trees); therefore, few studies on *S. vaninii* have been reported. Recently, several studies reported the anticancer (He et al., 2021a), anti-gout (Guo et al., 2021), anti-melanogenic and anti-wrinkle effects (Im et al., 2019) of extracts from *S. vaninii*. However, the bioactive components and the composition of extracts from *S. vaninii* remain to be further determined. Therefore, in this study, phenolic-rich extracts from *S. vaninii* (SHE) were prepared, and the phenolic profile and the main phenolic compound content of SHE were studied. The radical scavenging, anti-lipid peroxidation and anti-DNA damage capacity of SHE *in vitro* was determined. Moreover, the antiproliferative

Abbreviations: SHE, Phenolic-rich extracts from*S. vaninii*; TPC, Total polyphenol content; TFC, Total flavonoid content; TTC, Total triterpene content; TSC, Total sterol content.

* Corresponding author. Institute of Agro-Products Processing and Nuclear-Agricultural Technology, Hubei Academy of Agricultural Sciences, Wuhan, 430064, China.
E-mail addresses: yinchaomin@163.com, yinchaomin@hbaas.com (C. Yin).

https://doi.org/10.1016/j.crfs.2023.100519
Received 17 January 2023; Received in revised form 19 April 2023; Accepted 11 May 2023
Available online 19 May 2023

activity of SHE on HepG2 cells was evaluated with the cell cycle arrest phase and apoptosis rate.

2. Materials and methods

2.1. Materials and chemical reagents

S. vaninii fruiting bodies were purchased from Linfeng Fungus Industry Co., Ltd. (Changbai County, Jilin Province, China) in January 2021 and were identified by 16S rRNA sequencing. The standards of different polyphenols and flavonoids were purchased from Sigma–Aldrich Chemical Co., Ltd. (St. Louis, USA). Primary antibodies (anti-Bcl-2, anti-Bax, anti-caspase-9, anti-caspase-3 and anti-β-actin) and secondary antibodies (anti-rabbit/anti-mouse) were purchased from Proteintech Group, Inc (Wuhan, China). Other analytical grade chemicals were provided by Sinopharm Chemical Reagent Co., Ltd. (Beijing, China).

2.2. Obtaining the phenolic-rich extracts

The dried *S. vaninii* fruiting bodies were ground to a homogeneous powder (40 mesh). Phenolic-rich extracts from *S. vaninii* (SHE) were obtained according to the methods described by Huang et al. (2022) with some modification. 20.0 g of powder and 600 mL of 95% ethanol were mixed and stirred continuously for 30 min. Then, the mixture was sonicated at 450 W and 30 °C for 15 min. After centrifugation at 5000 r/min for 10 min, the supernatant was collected, and the residues were re-extracted twice under the same process. Then, the three supernatants were combined and concentrated using a vacuum rotary evaporator. Finally, the extracts were lyophilized to obtain SHE and stored at 4 °C. The ethanol solution of SHE was used for composition and antioxidant analysis while the dimethyl sulfoxide solution of SHE was used for HepG2 cell experiments.

2.3. Determination of total phenol, flavonoid, triterpene and sterol contents

2.3.1. Total polyphenol content (TPC) determination

According to the method described by Lin et al. (2017), the TPC of SHE was measured as follows: 100 μL of SHE solution (0.5 mg/mL) and 200 μL of Folin-Ciocalteu reagent (Solarbio Life Sciences Co., Ltd., Beijing, China) were mixed. After incubation at 25 °C for 5 min, 200 μL of 20% Na_2CO_3 solution (w/v) was added and incubated at 50 °C for 15 min. Finally, the absorbance of the mixture at 680 nm was measured with a SPARK multifunctional microplate reader (Shimadzu, Japan). The regression equation was y = 7.25x + 0.2396 (R^2 = 0.9909) according to the standard of gallic acid, and the TPC was expressed as mg gallic acid equivalents (GAE)/g dry extract weight (EW).

2.3.2. Total flavonoid content (TFC) determination

The TFC of the SHE was measured according to the method described by Liu et al. (2017). Briefly, 300 μL of 5% $NaNO_2$ solution (w/v) and 100 μL of SHE solution (0.5 mg/mL) were mixed and incubated at 25 °C for 5 min. After adding 300 μL of $AlCl_3$ solution (10%, w/v), the mixture was incubated for another 6 min at 25 °C. Then, 240 μL of distilled water and 200 μL of 1 M NaOH solution were added. Finally, the absorbance of the mixture at 510 nm was measured and the calibration curve (y = 0.2003x + 0.0379, R^2 = 0.9988) was calculated according to the standard of rutin. The TFC was expressed as mg rutin equivalents (RE)/g EW.

2.3.3. Total triterpene content (TTC) determination

The TTC of SHE was measured according to the standard (NY/T 3676-2020) of the Ministry of Agriculture of China. First, 300 μL of SHE solution (0.5 mg/mL) was heated to dryness, and then 0.8 mL of perchloric acid and 0.1 mL of vanillin-acetic acid solution (5%, w/v) were added and mixed. After incubation at 60 °C for 20 min, the mixture was immediately placed in an ice water bath, and 5.0 mL of acetic acid was added, followed by incubation at 25 °C for 10 min. Finally, the absorbance of the mixture at 550 nm was measured, and oleanolic acid was used for calibration curve calculation (y = 4.78x - 0.0358, R^2 = 0.9972). The TTC was expressed as mg oleanolic acid equivalents (OAE)/g EW.

2.3.4. Total sterol content (TSC) determination

The TSC of the SHE was measured with the method described by Gao et al. (2021). Briefly, 1.0 mL of SHE solution (0.5 mg/mL) and 1.0 mL of ferric chloride mix indicator (7.5 mM ferric chloride, solvent was a mixture of H_2O, H_3PO_4 and H_2SO_4 with a vol ratio of 1:6.7:88.5) were mixed and shaken vigorously. After standing at room temperature for 5 min, the absorbance of the mixture at 530 nm was measured, and ergosterol was used as a standard (y = 2.545x + 0.1048, R^2 = 0.9932). The TSC was expressed as mg ergosterol equivalents (EE)/g EW.

2.4. Identification and quantification of polyphenols using UPLC-Orbitrap-MS

Briefly, 50 μg of SHE was dissolved in 300 μL of methanol, and 5 μL of DL-4-chlorophenylalanine (1.0 mg/mL) was added as the internal standard. After vigorous shaking and centrifugation, the supernatant was collected before analysis. The analysis was performed on a Vanquish UPLC-Orbitrap-MS system (Thermo Fisher Scientific, Germany) equipped with a Waters HSS T3 column (50 mm × 2.1 mm, 1.8 μm). For identification of polyphenol and flavonoid, the mobile phases were 0.1% acetic acid aqueous solution (A) and acetonitrile with 0.1% acetic acid+0.1% isopropyl alcohol (B). The elution gradient was as follows: 0–2.0 min (90% A), 2.0–6.0 min (90-40% A), 6.0–15.0 min (40% A), and 15.0–17.0 min (water/acetonitrile = 90:10). For quantification of the main polyphenol and flavonoid, the mobile phases were 0.1% acetic acid aqueous solution (A) and acetonitrile with 0.1% acetic acid (B). The elution gradient was as follows: 0–2.0 min (90% A), 2.0–6.0 min (90-40% A), 6.0–8.0 min (40% A), 8.0–8.5 min (40%–5% A), and 8.5–12.0 min (5%–95% A) for phenolic acid separation and 0–12.0 min (90% A) for flavonoid separation. The injection volume was 2.0 μL, the flow rate was 0.3 mL/min, and the column oven was set at 40 °C. The parameters for Q Exactive hybrid Q-Orbitrap MS were set as follows: aux gas pressure, 10 arb; sheath gas pressure, 40 arb; capillary temperature, 320 °C; spray voltage, 2.8 kV (negative)/3.0 kV (positive). The scanning mode was full-scan MS2. The standard compounds used for quantification are shown in Table 2.

2.5. Antioxidant activities of SHE in vitro

2.5.1. Radical scavenging activity and reducing power

The ABTS, DPPH and hydroxyl radical scavenging activities as well as the reducing power of SHE were determined according to the method of Liu et al. (2017). SHE samples at different concentrations were assayed, and Vc was used as a control.

2.5.2. Lipid peroxidation inhibition activity

The lipid peroxidation inhibition activity was determined with the method of Liu et al. (2017). Briefly, 1 vol of egg yolks and 9 vol of ethanol were shaken vigorously. After centrifugation, the yolk suspension supernatant was collected. 1.0 mL of 250 mM $FeSO_4$ solution, 1.0 mL of SHE solution with different concentrations and 2.0 mL of the yolk suspension supernatant were mixed and immediately incubated in a water bath at 37 °C for 1 h. Then, 1.0 mL of 0.67% thiobarbituric acid (w/v) and 1.0 mL of 15% trichloroacetic acid (w/v) were added, followed by incubation at 100 °C for 40 min. After that, the supernatant was collected by centrifugation at 5000 rpm for 10 min, and the absorbance at 532 nm was measured. The lipid peroxidation inhibition activity was calculated according to Eq. (1):

Inhibition of lipid peroxidation (%) = $(A_0\text{-}A_1)/(A_0\text{-}A_2) \times 100\%$ (1)

where A_1, A_0 and A_2 represent the absorbance of the tested sample, control (without sample) and blank, respectively.

2.5.3. DNA damage inhibition activity

DNA damage inhibition activity was determined with pMD18-T plasmid DNA (Takara, Dalian, China). Plasmid DNA was damaged by H_2O_2 and $FeSO_4$ with the method described by Chen et al. (2021). In brief, 4.0 μL of different samples and 0.5 μg plasmid DNA were mixed. Then, 2.0 μL of 5% H_2O_2 solution (v/v) and 2.0 μL of 4.0 mM $FeSO_4$ solution were added. Finally, 50 mM phosphate buffer (pH 7.0) was added to bring the final volume to 15.0 μL. The mixture was incubated in a water bath at 37 °C for 30 min and then immediately placed in an ice bath for 10 min. After mixing with 10 × loading buffer, the samples were loaded into a 1.5% agarose gel containing 0.001% GelStain (TransGen, Beijing, China). Electrophoresis was performed in a horizontal slab in Tris-EDTA buffer at 70 V for 60 min. Under ultraviolet illumination, the gel was photographed and quantified using a GEL SensiAnsys system (Shanhai Peiqing Science & Technology Co., Ltd., China).

2.6. The antiproliferative activity of SHE

2.6.1. Cell culture

HepG2 cells were purchased from Wuhan Botao Biotechnology Co., Ltd. (Wuhan, China) and cultivated in DMEM/F-12 medium (HyClone, America) containing 50 U/mL streptomycin, 50 U/mL penicillin and 10% FBS (Sera & Pro, Germany). HepG2 cells were grown on petri dishes at 37 °C in an air-humidified incubator supplied with 5% CO_2.

2.6.2. MTT assay

The cytotoxicity of the SHE sample toward HepG2 cells was measured using the MTT method (Yin et al., 2022). Briefly, the cell density was adjusted to 5 × 10^3 cell/mL, and then, 200 μL of cell suspension was added to 96-well plates. The plates were cultured at 37 °C for 24 h in an air-humidified incubator supplied with 5% CO_2. Then, different SHE solutions were added to co-culture for 24 h and 48 h. Then, 20 μL of MTT solution was added and incubated for 4 h. Subsequently, MTT was removed and 150 μL of DMSO was added. Finally, the absorbance at 570 nm was recorded. The inhibition rate of HepG2 cells was calculated according to Eq. (2):

inhibition rate (%) = 1 - $(A_0\text{-}A_2)/(A_1\text{-}A_2) \times 100\%$ (2)

where A_0, A_1 and A_2 represent the absorbance of the treated, untreated and control groups, respectively.

2.6.3. Flow cytometric analysis of the cell cycle and apoptosis

HepG2 cells were cultured in a 6-well plate at a density of 5 × 10^3 cell/mL overnight and then treated with SHE solutions at different concentrations (0, 400, 800 and 1200 μg/mL) for 24 h. Then, the cells were collected, washed with ice-cold PBS solution and resuspended in 1 × binding buffer. Then, PI (10.0 μL) and Annexin V-FITC (5.0 μL) were added. After incubation in darkness at 25 °C for 15 min, the cells were immediately subjected to flow cytometry.

2.6.4. Western blot analysis

HepG2 cells were harvested, the cell cytoplasmic protein was extracted, and its concentration was determined. After dilution, proteins were loaded and separated by SDS–PAGE. Then, the proteins were transferred to PVDF membranes according to the manufacturer's instruction for the BioRad Transfer System. The PVDF membrane was placed in a sterile Petri dish and blocked with TBST solution (Tris buffer containing 0.1% Tween-20) with 5% skimmed milk at 25 °C for 1 h. Then, the membrane was washed three times and incubated with the primary antibody in TBST solution overnight at 4 °C. After washing three times, the membranes were probed with the secondary antibody in TBST solution at 25 °C for 1 h. After washing, an ECL kit (ApplyGen, Beijing, China) was used for band visualization.

2.7. Statistical analysis

Results were presented as means ± SD and three independent repetitions were conducted in each experiment. Comparisons were evaluated using Duncan's multiple range test and one-way analysis of variance test. $p < 0.05$ was considered statistically significant.

3. Results

3.1. The content of total phenols, total flavonoids, total triterpenes and total sterols in SHE

As shown in Table S1, the yield of SHE extracted from *S. vaninii* was 5.21% (w/w), which was higher than that of *Phellinus igniarius* (3.52%, w/w) (Zheng et al., 2019), but lower than that of *Inonotus sanghuang* (8.33%, w/w) (Liu et al., 2017). The TPC and TFC of SHE were 42.42 mg GAE/g EW and 8.50 mg RE/g EW, respectively. Lv et al. (2021) reported that the TPC and TFC in wild *S. vaninii* were 15.38 mg GAE/g EW and 13.58 mg RE/g EW, respectively. Obviously, the artificially cultivated *S. vaninii* in this study showed higher TPC but lower TFC than wild *S. vaninii*. Moreover, SHE showed high TTC and TSC, which were 6.70 mg OAE/g EW and 7.06 mg EE/g EW, respectively. Zhang et al. (2021) determined the TTC of artificially cultivated *S. vaninii* from different sources, and the TTC ranged from 5.61 to 26.29 mg OAE/g EW.

3.2. Identification of phenolic compounds in SHE

To identify the polyphenol composition in SHE, a high sensitivity and specificity UPLC-Orbitrap-MS was used to characterize these compounds. 14 phenolic acids, 8 flavonoids, 8 organic acids and fatty acids, and 2 terpenoids in SHE were characterized. Their molecular formula, retention time, molecular weight, MS/MS fragment ions and calculated mass (*m/z*) are listed in Table 1. The total ion chromatogram of SHE is shown in Fig. 1. Phenolic compounds were identified by comparison with MS data and the retention time of the standard compounds or MS/MS data and ESI-MS data in the MassBank and literatures.

3.2.1. Phenolic acids

Compared to the UV spectral and fragment ion characteristics of authentic standards, Compounds A1, A2, A3, A4, A5, A6, A7 and A14 were identified as gallic acid, protocatechuic acid, protocatechualdehyde, syringic acid, phthalic acid, p-coumaric acid, vanillic acid and caffeic acid. Compound A8 exhibited the molecular ion ($(M\text{-}H)^-$) at *m/z* 219 and generated a highly significant fragment at *m/z* 177 ($(M\text{-}H\text{-}C_2H_2O)^-$), which confirmed that this compound was hispolon (Zan et al., 2022). Compound A9 exhibited a molecular ion ($(M\text{-}H)^-$) at *m/z* 421, and the major fragments were *m/z* 379, *m/z* 241, *m/z* 217, *m/z* 175, and *m/z* 159; thus, Compound A9 was tentatively identified as interfungin B (Cui, 2022). Compound A10 showed the molecular ion $(M\text{-}H)^-$ at *m/z* 246 and two fragments at *m/z* 159 $(M\text{-}H\text{-}C_3H_2O_3)^-$ and *m/z* 201 $(M\text{-}H\text{-}CO_2)^-$; it was identified as hispidin, which had been described by Zan et al. (2022). Compound A11 exhibited the molecular ion $(M\text{-}H)^-$ at *m/z* 165 and its fragments at *m/z* 147 and *m/z* 119, probably due to the loss of H_2O and CO_2, respectively. Therefore, it was identified as benzenebutanoic acid. Compound A12 (*m/z* 208) showed two major fragments at *m/z* 161 $(M\text{-}H\text{-ethanol})^-$ and *m/z* 179 $(M\text{-}H\text{-}CO)^-$; thus, it was identified as ethyl caffeate (Barth et al., 2019). Compound A13 (*m/z* 453) generated six fragments at *m/z* 379, *m/z* 351, *m/z* 175, *m/z* 163, *m/z* 147 and *m/z* 137, and it was tentatively identified as phellibaumin E as reported by Wu et al. (2011).

Table 1
Detection and identification of main phenolic compounds in SHE by UPLC-Orbitrap-MS.

Identification		RT (min)	Formula	MW	[M-H]⁻(m/z)	[M+H]⁻(m/z)	Major fragmention (m/z)
Phenolic acids							
A1	Gallic acid	1.815	$C_7H_6O_5$	170	169.0146		125.02
A2	Protocatechuic acid	2.714	$C_7H_6O_4$	154	153.0195		109.03
A3	Protocatechualdehyde	4.079	$C_7H_6O_3$	138		139.0388	109.02, 137.04
A4	Syringic acid	4.588	$C_9H_{10}O_5$	198	197.0461		123.0, 167.0182.02
A5	Phthalic acid	4.619	$C_8H_6O_4$	166	165.0198		103.03, 137.01
A6	p-Coumaric acid	5.002	$C_9H_8O_3$	164	163.0405		93.02, 119.05
A7	Vanillic acid	5.043	$C_8H_8O_4$	168	167.0354		108.02, 123.04, 152.01
A8	Hispolon	5.233	$C_{12}H_{12}O_4$	220	219.0562		177.13
A9	Interfungin B	5.265	$C_{23}H_{18}O_8$	422	421.1068		159.01, 175.03, 217.02, 241.05, 379.08
A10	Hispidin	6.173	$C_{13}H_{10}O_5$	246	245.0459		159.23, 201.13
A11	Benzenebutanoic acid	6.255	$C_{10}H_{12}O_2$	164		165.0908	119.08, 147.08
A12	Ethyl caffeate	6.421	$C_{11}H_{12}O_4$	208	207.0667		135.04, 161.02, 179.03
A13	Phellibaumin E	6.511	$C_{24}H_{20}O_9$	452		453.1069	137.31, 147.21, 163.12, 175.24, 351.26, 379.31
A14	Caffeic acid	6.611	$C_9H_8O_4$	180		181.0387	135.04, 161.03
Flavonoids							
B1	Scoparone	3.032	$C_{11}H_{10}O_4$	206		207.0910	151.07
B2	Esculetin	4.471	$C_9H_6O_4$	178	177.0199		133.02, 177.01
B3	Taxifolin	5.027	$C_{15}H_{12}O_7$	304		305.0650	153.03, 259.05
B4	Naringenin chalcone	5.488	$C_{15}H_{12}O_5$	272	271.0613		151.05, 271.02
B5	Catechin	6.412	$C_{15}H_{14}O_6$	290		291.0752	125.02, 179.03, 205.07, 245.08, 289.07
B6	Nobiletin	7.780	$C_{21}H_{22}O_8$	402		403.1380	341.13, 355.12, 373.09
B7	Tangeretin	8.161	$C_{20}H_{20}O_7$	372		373.1275	312.23, 343.08, 373.12
B8	Emodin	8.520	$C_{15}H_{10}O_5$	270	269.0457		225.05, 269.04
Organic acids and fatty acids							
C1	Gamma-aminobutyric acid	0.735	$C_4H_9NO_2$	103		104.0709	69.08, 87.04
C2	Succinic acid	0.997	$C_4H_6O_4$	118	117.0193		73.02
C3	Sebacic acid	6.081	$C_{10}H_{18}O_4$	202	201.1137		139.11, 183.10
C4	Azelaic acid	8.316	$C_9H_{16}O_4$	188	187.0980		97.06, 125.09
C5	Alpha-linolenic acid	9.294	$C_{18}H_{30}O_2$	278		279.2314	67.05, 81.07, 95.08, 109.10
C6	Octadecanedioic acid	9.582	$C_{18}H_{34}O_4$	314	313.2387		251.23, 295.22
C7	Linoleic acid	10.019	$C_{18}H_{32}O_2$	280	279.2333		279.23
C8	Heneicosanoic acid	12.130	$C_{21}H_{42}O_2$	326	325.31190		183.01, 325.18
Terpenoids							
D1	Sterebin D	6.938	$C_{18}H_{30}O_3$	294		295.2187	219.22, 259.21, 277.28
D2	Phellilins C	9.217	$C_{18}H_{28}O_3$	292	291.2105		121.31, 125.26, 185.25, 197.34

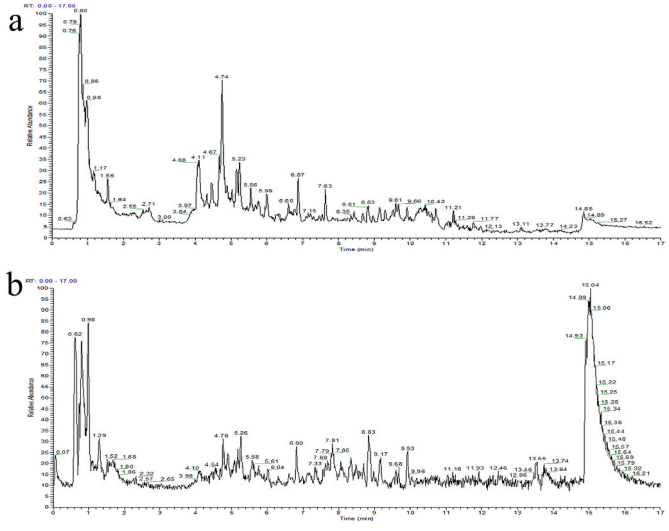

Fig. 1. UPLC-Orbitrap-MS negative ion (a) and positive ion (b) mass spectrum base compound ion flow from SHE.

3.2.2. Flavonoids

Based on the comparison of chromatographic retention time and fragment ions to the authentic standards, Compounds B3 and B5 were identified as taxifolin and catechin, respectively. Compound B1 showed the molecular ion (M-H)⁻ at *m/z* 207 and produced characteristic fragments at *m/z* 151. It was identified as scoparone, which was described by Zhao et al. (2020). Compound B2 exhibited the molecular ion (M-H)⁻ at *m/z* 177 and the characteristic fragments at *m/z* 133; it was identified as esculetin and had been described by Li et al. (2012). Compound B4 exhibited the molecular ion (M-H)⁻ at *m/z* 271 and produced main fragments at *m/z* 151; therefore, it was tentatively identified as naringenin chalcone according to the report of Lo Scalzo et al. (2021). According to the results of Wang et al. (2018), Compound B6 was identified as nobiletin, which yielded the molecular ion (M-H)⁻ at *m/z* 403 and three prominent fragments at *m/z* 373, *m/z* 355 and *m/z* 341. Compound B7 was tentatively identified as tangeretin due to its molecular ion (M-H)⁻ at *m/z* 373 and three characteristic fragments at *m/z* 373, *m/z* 343 and *m/z* 312 (Wang et al., 2018). Compound B8, with the molecular ion (M-H)⁻ at *m/z* 269, yielded prominent fragment ions at *m/z* 225 by deprotonated CO_2 (Koyama et al., 2009). Therefore, it was tentatively identified as emodin.

3.2.3. Organic acids and fatty acids

By comparison with the MassBank and ChemSpider databases, Compound C1, C2, C3, C5, C6, C7, and C8 were tentatively identified as gamma-aminobutyric acid, succinic acid, sebacic acid, alpha-linolenic acid, octadecanedioic acid, linoleic acid and heneicosanoic acid. Compound C4 exhibited the molecular ion (M-H)⁻ at *m/z* 373 and yielded two characteristic fragments at *m/z* 125 and *m/z* 97, thus, it was identified as azelaic acid (Zengin et al., 2018).

3.2.4. Other compounds

Compound D1 exhibited a molecular ion (M-H)⁻ at *m/z* 295 and three major fragments at *m/z* 277, *m/z* 259, and *m/z* 259, which was consistent with the report of Formigoni et al. (2018); thus, Compound D1 was identified as Sterebin D and it belonged to diterpene. Compound D2 with the molecular ion (M-H)⁻ at *m/z* 291 and four characteristic fragments at *m/z* 121, *m/z* 125, *m/z* 185, and *m/z* 197 was identified as phellilins C according to the literature reported by Zheng et al. (2022), and it

belonged to sesquiterpenes.

3.3. Quantitative analysis of the main polyphenols and flavonoids in SHE

The major polyphenols and flavonoids in SHE were quantified by UPLC-Orbitrap-MS, and the chromatograms are shown in Fig. S1. As presented in Table 2, SHE had higher contents of protocatechualdehyde (394.68 μg/g), protocatechuic acid (196.88 μg/g), caffeic acid (96.11 μg/g) and L-phenylalanine (12.72 μg/g). Moreover, the contents of other polyphenols including *p*-coumaric acid, vanillic acid, gallic acid, and syringic acid, ranged from 1.27 to 5.09 μg/g. However, syringaldehyde, trans-ferulic acid, benzoic acid, salicylic acid, 4-hydroxy-3,5-dimethoxycinnamic acid, hydrocinnamic acid and trans-cinnamic acid were not detected. Except for polyphenols, two flavonoid, catechin and (+)-taxifolin, were detected, with contents of 0.12 μg/g and 8.59 μg/g, respectively. However, most flavonoid, including dihydromyricetin, L-epicatechin, rutin, vitexin, quercetin-3-β-D-glucoside, quercitrin, (+)-dihydrokaempferol, luteolin, quercetin, naringenin chalcone, apigenin, kaempferol and isorhamnetin, were not detected in SHE.

3.4. Antioxidant activity of SHE

Phenolic acids and flavonoid are the main compounds that exert antioxidant activity in many mushrooms (Liu et al., 2017). Therefore, the antioxidant activity including radical scavenging activity, reducing power, anti-lipid peroxidation capacity and anti-DNA damage activity of SHE *in vitro* was determined.

Table 2
Quantitative analysis of main polyphenols and flavonoids in SHE.

Standards	RT (min)	Standard curve line	R^2 Value	Content (μg/g)
Polyphenols				712.84
Gallic acid	0.960	$Y = 5.896e^3X$	0.9993	1.68 ± 0.02
L-Phenylalanine	1.050	$Y = 5.238e^4X$	0.9933	12.72 ± 0.02
Protocatechuic acid	1.730	$Y = 1.127e^5X$	0.9994	196.88 ± 0.26
Protocatechualdehyde	2.910	$Y = 1.709e^5X$	0.9951	394.68 ± 1.51
Vanillic acid	3.980	$Y = 1.188e^5X$	0.9990	4.41 ± 0.03
Caffeic acid	4.120	$Y = 1.636e^5X$	0.9991	96.11 ± 0.87
Syringic acid	4.380	$Y = 1.117e^5X$	0.9983	1.27 ± 0.02
4-Hydroxybenzoic acid	4.990	$Y = 2.169e^4X$	0.9989	–
p-Coumaric acid	5.140	$Y = 3.222e^5X$	0.9976	5.09 ± 0.04
Syringaldehyde	5.350	$Y = 9.326e^4X$	0.9973	–
Salicylic acid	5.410	$Y = 1.333e^5X$	0.9980	–
Trans-Ferulic acid	5.530	$Y = 8.323e^4X$	0.9985	–
4-Hydroxy-3,5-dimethoxycinnamic acid	5.590	$Y = 9.366e^4X$	0.9989	–
Benzoic acid	5.870	$Y = 7.738e^4X$	0.9975	–
Hydrocinnamic acid	7.000	$Y = 1.166e^5X$	0.9988	–
Trans-Cinnamic acid	7.100	$Y = 1.616e^5X$	0.9989	–
Flavonoids				8.71
Catechin	3.750	$Y = 7.342e^4X$	0.9986	0.12 ± 0.01
Dihydromyricetin	4.660	$Y = 5.418e^4X$	0.9956	–
L-Epicatechin	4.660	$Y = 7.562e^4X$	0.9980	–
Rutin	5.510	$Y = 9.22e^4X$	0.9977	–
Vitexin	5.530	$Y = 9.825e^4X$	0.9991	–
Quercetin-3-β-D-glucoside	5.650	$Y = 1.005e^5X$	0.9985	–
(+)-taxifolin	5.690	$Y = 9.112e^4X$	0.9993	8.59 ± 0.05
Quercitrin	6.000	$Y = 6.337e^4X$	0.9987	–
(+)-dihydrokaempferol	6.300	$Y = 1.225e^5X$	0.9991	–
Luteolin	6.940	$Y = 1.435e^5X$	0.9974	–
Quercetin	6.970	$Y = 1.419e^5X$	0.9973	–
Naringenin chalcone	7.450	$Y = 1.51e^5X$	0.9991	–
Apigenin	7.470	$Y = 2.17e^5X$	0.9981	–
Kaempferol	7.560	$Y = 1.175e^5X$	0.9963	–
Isorhamnetin	7.640	$Y = 1.515e^5X$	0.9970	–

3.4.1. Radical scavenging activity and reducing power

ABTS, DPPH and HO• radicals have been commonly used for evaluating the antioxidant activity of natural bioactive compounds (Lin et al., 2022). As shown in Fig. 2a–c, SHE showed strong scavenging activities toward ABTS and DPPH radicals but relatively moderate scavenging ability toward HO• radicals, and the scavenging rate on ABTS, DPPH and HO• radicals increased with increasing concentration. At the concentration of 2.5 mg/mL, the scavenging rates of SHE on ABTS, DPPH and hydroxyl radicals were 99.34%, 86.96% and 29.40%, respectively. Lv et al. (2021) reported that ethanolic extract from wild *S. vaninii* showed high DPPH radicals scavenging activity, and the scavenging rate was as high as that of butylhydroxyanisole at the concentration of 1.6 mg/mL, which was consistent with our results. Reducing power is another indicator of antioxidant capacity, and the reducing power of SHE showed a manner of concentration-dependence, but it was lower than that of Vc at the same concentration (Fig. 2d).

3.4.2. Lipid peroxidation inhibition activity

Lipid peroxidation is the outcome of free radicals attacking unsaturated fatty acids. Lipid peroxide, the product of lipid peroxidation, usually decomposes to form aldehydes to cross-link or change the structures of carbohydrates, DNA, proteins or lipids, causing a variety of aging diseases (Lin et al., 2022). As shown in Fig. 2e, SHE and Vc showed excellent lipid peroxidation inhibition activity in a concentration-dependent manner. At the concentration of 2.5 mg/mL, the lipid peroxidation inhibition activity of SHE and Vc were 75.16% and 49.06%, respectively. The IC50 of SHE and Vc were determined to be 1.247 mg/mL and 2.647 mg/mL, respectively. The results showed that SHE had strong lipid peroxidation inhibition activity.

3.4.3. DNA damage inhibition activity

The inhibitory activity of SHE on DNA damage induced by the coaction of H_2O_2 and Fe^{2+} (Chen et al., 2021) was determined using the pMD18-T plasmid. Fig. 2f shows the electrophoretic pattern of oxidized DNA with or without SHE at different concentrations. pMD18-T plasmid DNA showed the band of supercoiled DNA form on agarose gel (Lane 1). The supercoiled DNA was damaged by the Fenton reaction to form open circular DNA (Lane 2). Lanes 3–5 revealed that SHE at concentrations of 0.25, 0.5 and 2.0 mg/mL suppressed open circular DNA formation. Fig. 2g shows the relative content of supercoiled DNA and open circular DNA in different groups. Obviously, the relative content of open circular DNA was reduced with the increased concentration of SHE. At the concentration of 2.0 mg/mL (Group 5), the relative content of open circular DNA was 25.91%, which was 43.98% lower than that of the blank control group (Group 2). Our results showed that SHE had strong anti-DNA damage capacity.

3.5. Antiproliferative activities of SHE on HepG2 cells

3.5.1. Effects of SHE on HepG2 cells viability

The antiproliferation ability of SHE on HepG2 cells is shown in Fig. 3a. Cell viability was inhibited by high concentrations of SHE in a dose-dependent manner. When the cells were treated with SHE (1200 μg/mL) for 24 h or 48 h, the cell viability reached 53.20% and 52.46%, respectively. The results suggested that SHE exerted cytotoxic effects and inhibited the growth of HepG2 cells. Moreover, it seems that the treatment time has little impact on the cell viability rate. Interestingly, Lin et al. (2017) reported that the ethanolic extracts from *S. vaninii*, *S. baumii* and *S. sanghuang* showed a certain growth inhibition effect on HepG2 cells, and *S. sanghuang* ethanolic extracts showed the lowest viability rates of 46.7% at a concentration of 500 μg/mL. Liu et al.

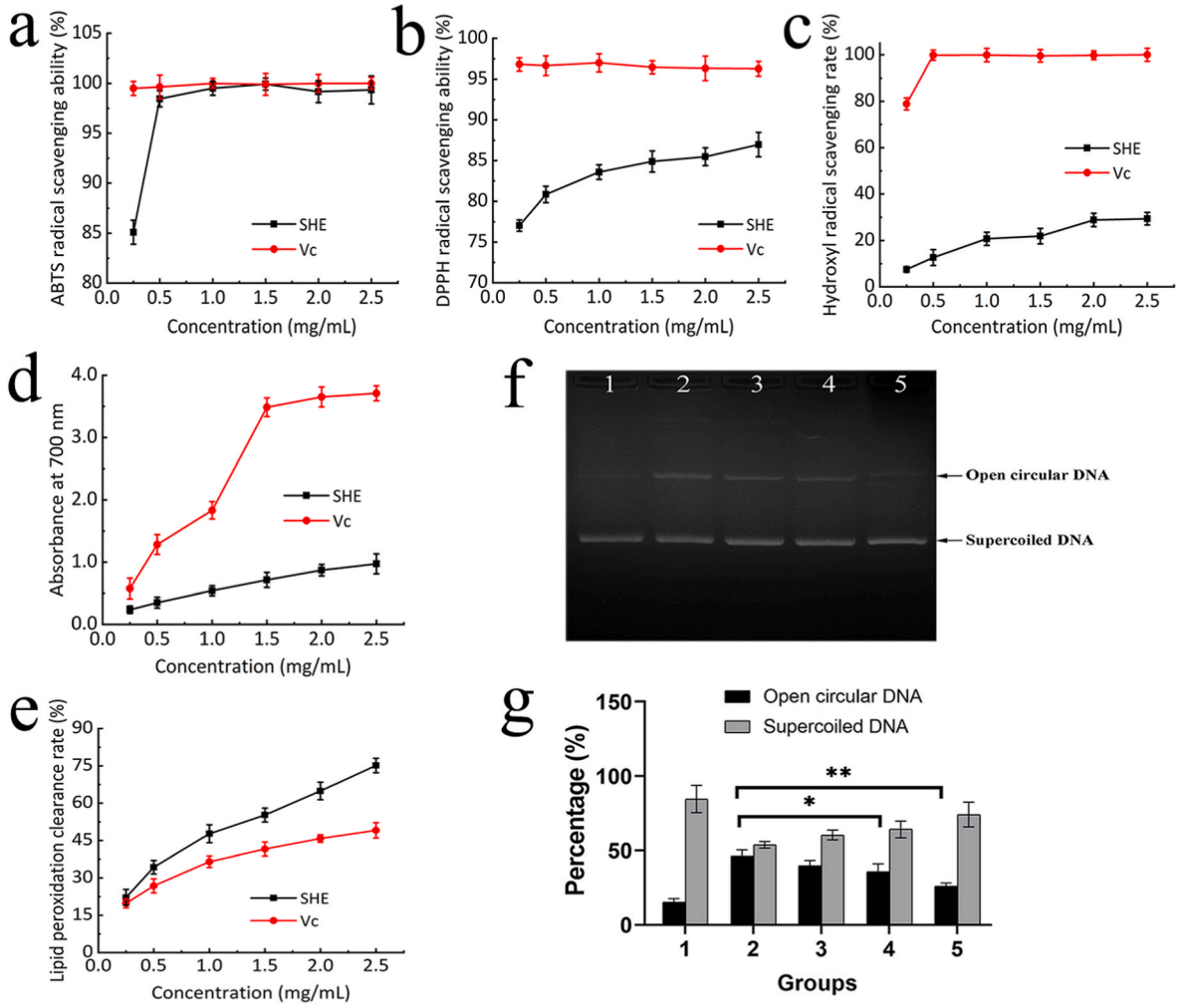

Fig. 2. Antioxidant activity of SHE. (a: ABTS radical scavenging capacity; b: DPPH radical scavenging activity; c: hydroxyl radical scavenging activity; d: reducing power; e: anti-lipid peroxidation capacity; f: electrophoretic agarose gel of plasmid DNA after incubation with $FeSO_4$ and H_2O_2 in presence or absence of SHE. Lane 1: control; lane 2: blank control; lane 3: 0.25 mg/mL SHE; lane 4: 0.5 mg/mL SHE; lane 5: 2.0 mg/mL SHE. g: the relative percentage of supercoiled DNA and open circular DNA in different groups.)

(2017) and Zan et al. (2022) reported that the IC_{50} values of ethyl acetate extracts from *S. sanghuang* and *S. baumii* on HepG2 cells were 308.5 μg/mL and 238.3 μg/mL, respectively. Another study found that the ethanolic extracts from *S. vaninii* significantly inhibited the growth of SiHa, SK-OV-3 and SGC-7901 cells, and their IC50 values were 71.80, 89.60 and 116.00 μg/mL, respectively (He et al., 2021a). These results certified that the organic solvent extracts from *Sanghuangporus* may have a certain antiproliferation effect on tumor cells. As the main bioactive compounds in these extracts, polyphenols may exert an important role. In addition, the morphology of HepG2 cells treated with SHE at different concentrations for 48 h is shown in Fig. 3b. The HE staining results demonstrated that the number of HepG2 cells decreased gradually with increasing SHE concentration.

3.5.2. Effects of SHE on the apoptosis of HepG2 cells

As shown in Fig. 3c and d, after treatment with SHE at different concentrations for 48 h, the ratio of apoptotic cells obviously increased in the phases of early apoptosis (from 2.89% to 21.27%) and late apoptosis (from 3.01% to 6.93%). The data indicated that SHE could induce apoptosis of HepG2 cells in a concentration-dependent manner, which was consistent with the MTT results. The results demonstrated that the antiproliferative effect of SHE on HepG2 cells may be attributed to its apoptosis-inducing activity. Similarly, a dichloromethane extract from *S. vaninii* (DCMPI) (Dzah et al., 2021) and a pyrone compound from *S. vaninii* (Inoscavin A) (Qiu et al., 2022) exhibited apoptosis-inducing effects in HT-29 cells.

3.5.3. Effects of SHE on the cell cycle of HepG2 cells

The distribution of HepG2 cells in different phases was determined by flow cytometry, and the results are shown in Fig. 3e and f. The G0/G1 phase significantly accumulated, and the percentage of cells in this phase increased from 57.72% to 69.05% after treatment with SHE, but the percentage had no correlation with the concentration of SHE. At the same time, the percentage of cells in S phase significantly decreased from 31.48% to 13.09% in a concentration-dependent manner. The results showed that SHE arrested the cell cycle of HepG2 cells in G0/G1 phase. Similarly, *S. vaninii* ethanolic extracts exhibited the apoptosis-inducing effects via G0/G1 phase arrest in B16F10 melanoma cells (Park, 2014) and SiHa cells (He et al., 2021a).

3.5.4. Apoptosis-regulated proteins expression of HepG2 cells

In order to analyze the apoptosis signaling, the relative expression levels of apoptosis-related proteins were measured before and after exposure to SHE at different concentrations by Western blot experiments. As shown in Fig. 4, the content of Bax protein significantly increased, while Bcl-2 protein content significantly decreased in a dose-dependent manner after treatment with SHE, resulting in a remarkable decrease in the protein ratio of Bcl-2/Bax. As shown in Fig. 4d and f, the

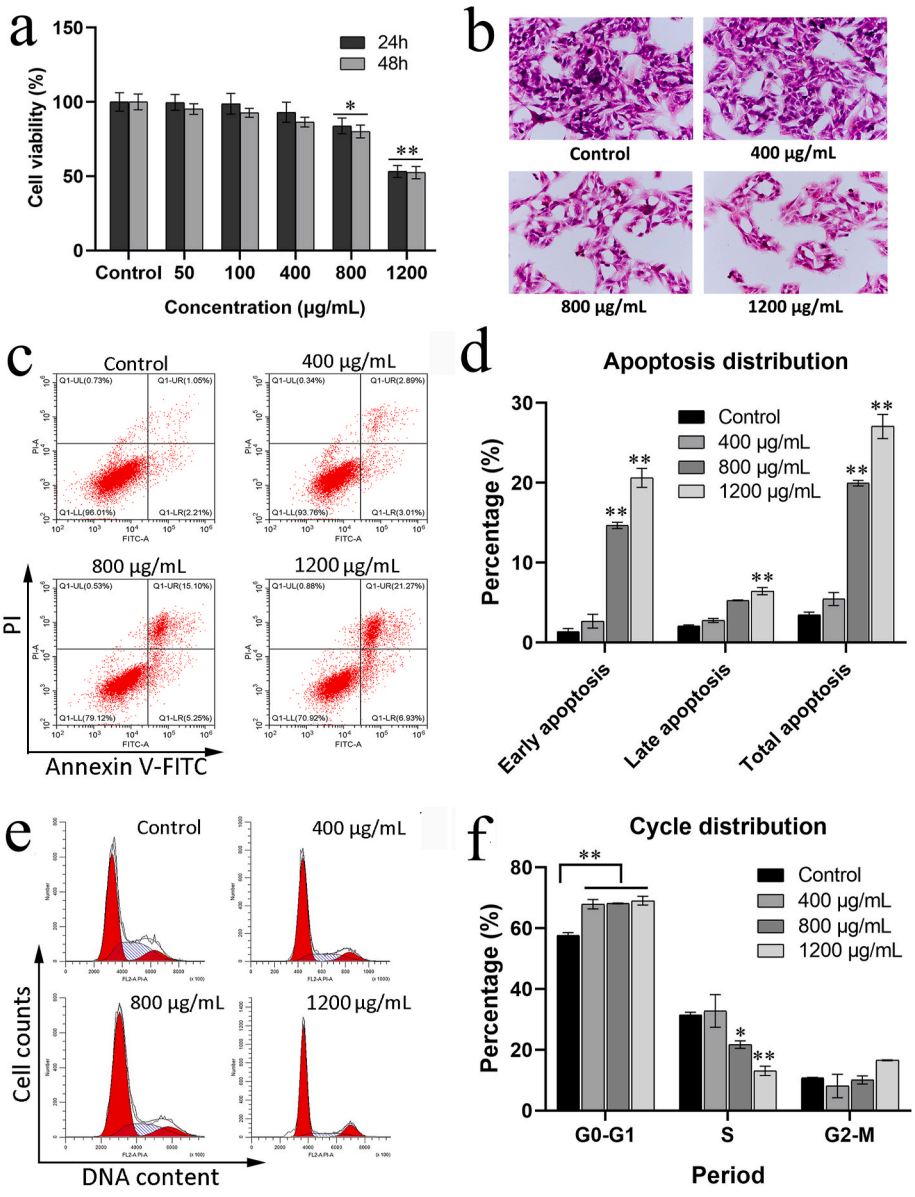

Fig. 3. The anti-proliferation effect of SHE on HepG2 cells. a: HepG2 cell viability, after treated with SHE at different concentrations for 24 and 48 h; b: the HE staining (20 ×) of HepG2 cells, treated with SHE at different concentrations for 48 h; c: HepG2 cell apoptosis ratio, after treated with SHE at different concentrations for 48 h; d: apoptosis distribution in different groups; e: cell cycle phase distribution of HepG2 cells, after treated with SHE at different concentration for 48 h; f: cell cycle distribution in different groups.

relative levels of cleaved caspase-9 and caspase-3 dramatically increased in a concentration-dependent manner in HepG2 cells after SHE treatment. This implies that the apoptosis-inducing effects of SHE on HepG2 cells may be attributed to the triggering of the caspases-dependent mitochondrial apoptotic pathway. Similarly, the apoptosis-inducing effects of *S. vaninii* ethanolic extracts in gastric cancer SGC-7901 cells and cervical cancer SiHa cells were mediated through the caspases-dependent mitochondrial apoptotic pathway (He et al., 2021a).

4. Discussion

Current studies have shown that *Sanghuangporus* fungi exhibit good pharmacological activities, including improved blood circulation, immunity enhancement, anti-inflammation, antibacterial, antioxidant and antitumor activities, due to their plentiful bioactive components, such as polyphenols, polysaccharides, triterpenoids, furanones and pyrans (Guo et al., 2021). To date, more than 100 chemical compounds from mycelia, fruiting bodies or fermentation broth of *Sanghuangporus* fungi have been isolated and identified (He et al., 2021b).

Polyphenols are one of the most important bioactive compounds in *Sanghuangporus* fungi, and they have strong antioxidant activity due to their phenolic hydroxyl groups (Cheng et al., 2022). In this study, 14 phenolic compounds were identified, including gallic acid, protocatechuic acid, protocatechualdehyde, vanillic acid, caffeic acid, etc., common phenolic compounds in *Sanghuangporus*. Among these, protocatechualdehyde (394.68 μg/g), protocatechuic acid (196.88 μg/g) and caffeic acid (96.11 μg/g) showed higher contents than the other detected phenolic compounds. In addition, we also found that protocatechualdehyde, protocatechuic acid and caffeic acid had high peak areas during polyphenol identification by UPLC-Orbitrap-MS. These results verified that protocatechualdehyde, protocatechuic acid and caffeic acid could be the main polyphenols in artificially cultivated *S. vaninii*. It has been reported that the fruiting bodies of *S. baumii*, *S. vaninii* and *S. sanghuang* as well as the mycelium of *S. sanghuang* all contain high contents of protocatechuic acid and protocatechualdehyde, among which the contents of protocatechuic acid and protocatechualdehyde in *S. vaninii* are as high as 41.5 μg/mg and 8.50 μg/mg, respectively (Lin et al., 2017). Chang et al. (2011) and Lee et al. (2015) respectively reported that the protocatechualdehyde and caffeic acid isolated from *Phellinus gilvus* and *P. linteus* exhibited higher antioxidant activity than the antioxidants of BHA and Trolox.

In addition to common phenolic compounds, some characteristic

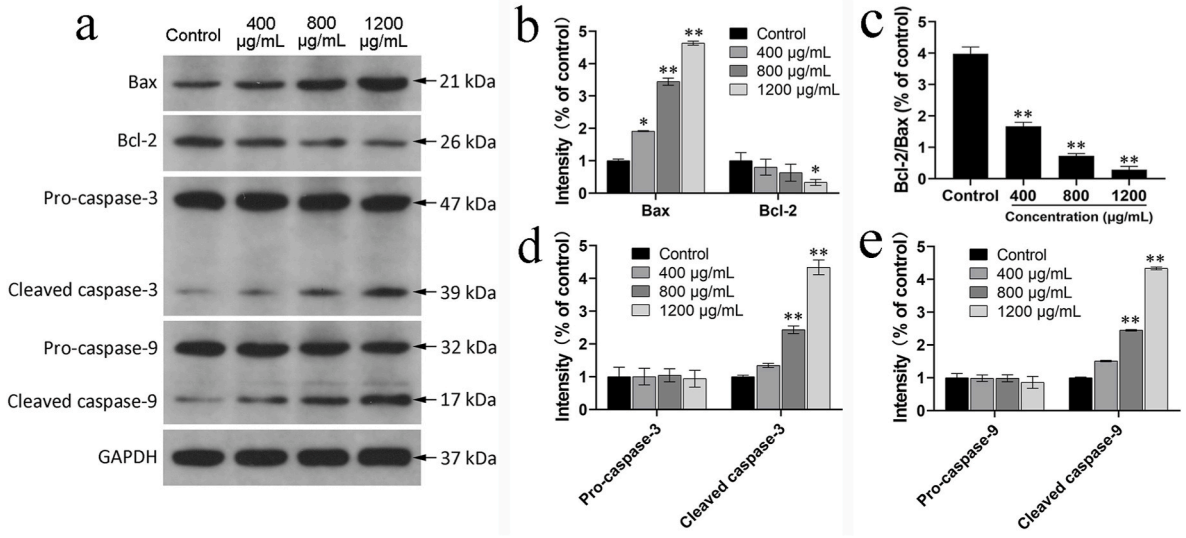

Fig. 4. The relative level of Bax, Bcl-2, pro-caspase-3, cleaved caspase-3, pro-caspase-9 and cleaved caspase-9 were analyzed by Western blot. a: Western blot; b: the relative intensity of Bax and Bcl-2 in different groups; c: the Bcl-2/Bax ratio in different groups; d: the relative intensity of pro-caspase-3 and cleaved caspase-3 in different groups; e: the relative intensity of pro-caspase-9 and cleaved caspase-9 in different groups.

polyphenols in *Sanghuangporus* fungi including hispolon, hispidin and phellibaumin E (Cheng et al., 2022) were identified in our study. Hispolon has a styrylpyrone structure, while hispidin has multiple hydroxyl structures, and phellibaumin E is a derivative of hispidin that possesses strong antioxidant activity (Chen et al., 2014). Jiang et al. (2020) demonstrated that the hispidin from *P. baumii* mycelia showed strong radical scavenging ability toward DPPH and TEAC, equivalent to vitamin C values of 89.41% and 75.98%, respectively. Chen et al. (2012) found that hispidin from *P. linteus* significantly inhibited peroxynitrite-induced DNA damage and reduced hydroxyl radicals' formation at doses of 10–20 μg/mL. In our study, SHE showed high scavenging activity toward ABTS and DPPH radicals as well as strong inhibition ability of lipid peroxidation and DNA damage. These could be attributed to the main phenolic compounds including protocatechualdehyde, protocatechuic acid, caffeic acid and hispidin.

Anticancer activity is another important pharmacological activity of polyphenols. Several phenolic compounds in *Sanghuangporus* fungi have been shown to have antiproliferation or anticancer activity; for example, Zhong et al. (2020) certified that protocatechualdehyde, the main phenolic component of *P. gilvus*, induced murine B16–F10 cell apoptosis and arrested the cell cycle in the G0/G1 phase. Chien et al. (2022) certified that protocatechualdehyde from *S. sanghuang* could effectively inhibit the growth of HepG2 cells at a low dose of 12.5 μg/mL. However, the most important anticancer bioactive compound in *Sanghuangporus* fungi could be hispolon, which is known as a cancer killer due to its strong and broad anticancer properties (Sarfraz et al., 2020; Chen et al., 2014). It has been reported that hispolon has the potential to arrest the cell cycle at the G0/G1 and G2/M phases in several cancer cells, such as A549, H661, DU145 and U87MG cells, and it sensitizes cancer cells by regulating the expression of caspase-9, -8 and -3, Bax and Bcl-2 protein (Sarfraz et al., 2020). In our study, SHE arrested the cell cycle of HepG2 cells in G0/G1 phase (Fig. 3f). It is well known that the G0/G1 phase is an important period for ribosome and RNA synthesis, while the S phase is a period for DNA replication. The accumulation of G0/G1 phase in HepG2 cells implied that SHE may disrupt the process of energy or substance preparation in HepG2 cells. Moreover, SHE treatment significantly decreased the protein ratio of Bcl-2/Bax and dramatically increased the relative content of cleaved caspase-9 and caspase-3 (Fig. 4). The decreased Bcl-2/Bax protein ratio certified that SHE may exert a pro-apoptotic effect by regulating the expression of apoptosis proteins in HepG2 cells. Increasing evidence indicates that upregulating Bax and downregulating Bcl-2 expression can trigger mitochondrial dysfunction, which will result in the release of cyt *c* to form apoptosomes and then activate downstream caspase-9 and caspase-3 in turn, thus resulting in cell apoptosis (Yu et al., 2022). The results showed that SHE could effectively induce HepG2 cell apoptosis via the caspases-dependent mitochondrial apoptotic pathway. Apparently, the antiproliferation activity of SHE could be attributed to the main phenolic components including hispolon and protocatechualdehyde. Whether the ingredients influence each other, resulting in a high inhibition dose, requires further study.

5. Conclusion

A phenolic-rich fraction from *S. vaninii* (SHE) was prepared, and the phenolic profile of SHE was identified in this study. The main polyphenols of SHE included protocatechualdehyde (394.68 μg/g), protocatechuic acid (196.88 μg/g), caffeic acid (96.11 μg/g), L-phenylalanine (12.72 μg/g), (+)-taxifolin (8.59 μg/g) and *p*-coumaric acid (5.09 μg/g). Moreover, SHE showed strong antioxidant activity and antiproliferative activity toward HepG2 cells. Taken together, the present study suggests the possibility of using *S. vaninii* as a valuable source of natural antioxidative and antiproliferative ingredients.

CRediT authorship contribution statement

Hong Gao: Writing – review & editing. **Chaomin Yin:** Writing – review & editing, Methodology. **Chen Li:** Data curation, Investigation, Methodology. **Yuhong Li:** Data curation, Investigation, Methodology. **Defang Shi:** Investigation, Validation. **Xiuzhi Fan:** Investigation, Validation. **Fen Yao:** Investigation, Validation. **Wenjing Wu:** Validation. **Jiangtao Li:** Validation.

Declaration of competing interest

The authors declare that they have no known competing financial interests or personal relationships that could have appeared to influence the work reported in this paper.

Data availability

Data will be made available on request.

Acknowledgments

This work was supported by grants from the National Natural Science Foundation of China (No. 31801921 & 32072229). Young-aged Top-notch Talent Training Program of Hubei Academy of Agricultural Sciences (2022). Special Project for Science and Technology Innovation of Wuhan (2022020801010343). Project of Edible Fungus Industrial Technology System of Hubei Province (HBHZDZB-2021-023).

Appendix A. Supplementary data

Supplementary data related to this article can be found at https://doi.org/10.1016/j.crfs.2023.100519.

References

Barth, C.D.S., Souza, H.G.T.D., Rocha, L.W., Madeira, C.R.D.S., Bresolin, T.M.B., 2019. RP-HPLC and LC–MS–MS determination of a bioactive artefact from *Ipomoea pes-caprae* extract. Rev. Bras. Farmacogn. 29 (5), 570–577.

Chang, Z.Q., Gebru, E., Lee, S.P., Rhee, M.H., Kim, J.C., Cheng, H., Park, S.C., 2011. *In vitro* antioxidant and anti-inflammatory activities of protocatechualdehyde isolated from *Phellinus gilvus*. J. Nutr. Sci. Vitaminol. 57 (1), 118–122.

Chen, S., Wang, X., Cheng, N., 2021. Ultrasound-assisted ethanol extraction of *Actinidia arguta* pollen possesses antioxidant activity and protects DNA from oxidative damage. J. Food Biochem. 45 (4), e13603.

Chen, W., Feng, L., Huang, Z., Su, H., 2012. Hispidin produced from *Phellinus linteus* protects against peroxynitrite-mediated DNA damage and hydroxyl radical generation. Chem. Biol. Interact. 199 (3), 137–142.

Chen, W., Shen, Y., Su, H., Zheng, X., 2014. Hispidin derived from *Phellinus linteus* affords protection against acrylamide-induced oxidative stress in Caco-2 cells. Chem. Biol. Interact. 219, 83–89.

Cheng, W.C., Yang, Y., Zhang, J.S., Li, Z.P., Lu, B.K., Wang, K., 2022. Recent advances in bioactive metabolites from 'Sanghuang' mushrooms. Acta Edulis Fungi. 27, 188–201 (in Chinese).

Chien, L.H., Deng, J.S., Jiang, W.P., Chen, C.C., Chou, Y.N., Lin, J.G., Huang, G.J., 2022. Study on the potential of *Sanghuangporus sanghuang* and its components as COVID-19 spike protein receptor binding domain inhibitors. Biomed. Pharmacother. 153, 113434.

Cui, S. Y, 2022. Research of the Constituent Characterization of *Phellinus Baumii* Polyphenols and its Antitumor Mechanism [Master's thesis]. [Hangzhou (ZJ)]. Zhejiang University.

Dzah, C.S., Duan, Y., Zhang, H., Ma, H., 2021. Effects of pretreatment and type of hydrolysis on the composition, antioxidant potential and HepG2 cytotoxicity of bound polyphenols from Tartary buckwheat (*Fagopyrum tataricum* L. Gaerth) hulls. Food Res. Int. 142, 110187.

Formigoni, M., Milani, P.G., da Silva Avíncola, A., Dos Santos, V.J., Benossi, L., Dacome, A.S., Pilau, E.J., da Costa, S.C., 2018. Pretreatment with ethanol as an alternative to improve steviol glycosides extraction and purification from a new variety of stevia. Food Chem. 241, 452–459.

Gao, S.X., Wang, Q., Guo, Y.F., Guo, P., Chen, P., Li, Y., 2021. The optimization of cellulose extraction of sterols from *Volvariella volvacea* by response surface methodology. J. Fungal Res. 19, 163–169 (in Chinese).

Guo, Q., Zhao, L., Zhu, Y., Wu, J., Hao, C., Song, S., Shi, W., 2021. Optimization of culture medium for *Sanghuangporus vaninii* and a study on its therapeutic effects on gout. Biomed. Pharmacother. 135, 111194.

He, P.Y., Hou, Y.H., Yang, Y., Li, N., 2021a. The anticancer effect of extract of medicinal mushroom *Sanghuangporus vaninii* against human cervical cancer cell via endoplasmic reticulum stress-mitochondrial apoptotic pathway. J. Ethnopharmacol. 279, 114345.

He, P., Zhang, Y., Li, N., 2021b. The phytochemistry and pharmacology of medicinal fungi of the genus *Phellinus*: a review. Food Funct. 12 (5), 1856–1881.

Huang, D., Li, C., Chen, Q., Xie, X., Fu, X., Chen, C., Huang, Q., Huang, Z., Dong, H., 2022. Identification of polyphenols from *Rosa roxburghii* Tratt pomace and evaluation of *in vitro* and *in vivo* antioxidant activity. Food Chem. 377, 131922.

Im, K.H., Baek, S.A., Choi, J., Lee, T.S., 2019. Antioxidant, anti-melanogenic and anti-wrinkle effects of *Phellinus vaninii*. MYCOBIOLOGY 47 (5), 1–12.

Jiang, F., Zhang, H.N., Zhang, L., Feng, J., Wang, W.H., Zhang, Z., Musa, A., Wu, D., Yang, Y., 2020. Antioxidant and neuroprotector influence of endo-polyphenol extract from magnesium acetate multi-stage addition in the oak bracket medicinal mushroom, *Phellinus baumii* (Agaricomycetes). Int. J. Med. Mushrooms 22 (2), 183–195.

Koyama, J., Takeuchi, A., Morita, I., Nishino, Y., Shimizu, M., Inoue, M., Kobayashi, N., 2009. Characterization of emodin metabolites in Raji cells by LC-APCI-MS/MS. Bioorg. Med. Chem. 17 (21), 7493–7499.

Lee, M.S., Hwang, B.S., Lee, I.K., Seo, G.S., Yun, B.S., 2015. Chemical constituents of the culture broth of *Phellinus linteus* and their antioxidant activity. MYCOBIOLOGY 43 (1), 43–48.

Li, Y.Y., Song, Y.Y., Liu, C.H., Huang, X.T., Zheng, X., Li, N., Xu, M.L., Mi, S.Q., Wang, N. S., 2012. Simultaneous determination of esculin and its metabolite esculetin in rat plasma by LC-ESI-MS/MS and its application in pharmacokinetic study. J. Chromatogr. B 907, 27–33.

Lin, W.C., Deng, J.S., Huang, S.S., Wu, S.H., Lin, H.Y., Huang, G.J., 2017. Evaluation of antioxidant, anti-inflammatory and anti-proliferative activities of ethanol extracts from different varieties of Sanghuang species. RSC Adv. 7 (13), 7780–7788.

Lin, Y., Pi, J., Jin, P., Liu, Y., Mai, X., Li, P., Fan, H., 2022. Enzyme and microwave co-assisted extraction, structural characterization and antioxidant activity of polysaccharides from Purple-heart Radish. Food Chem. 372, 131274.

Liu, K., Xiao, X., Wang, J., Chen, C., Hu, H., 2017. Polyphenolic composition and antioxidant, antiproliferative, and antimicrobial activities of mushroom *Inonotus sanghuang*. LWT–Food Sci. Technol. 82, 154–161.

Lo Scalzo, R., Florio, F.E., Fibiani, M., Speranza, G., Rabuffetti, M., Gattolin, S., Toppino, L., Rotino, G.L., 2021. Scrapped but not neglected: insights into the composition, molecular modulation and antioxidant capacity of phenols in peel of eggplant (*Solanum melongena* L.) fruits at different developmental stages. Plant Physiol. Biochem. 167, 678–690.

Lv, G.Y., Song, T.T., Cai, W.M., Zhang, Z.F., 2021. Comparative study of chemical components and antioxidant activities of wild *Sanghuangporus sanghuang* and *Sanghuangporus vaninii*. Mycosystema 40, 1833–1843 (in Chinese).

Park, H.J., 2014. CARI III inhibits tumor growth in a melanoma-bearing mouse model through induction of G0/G1 cell cycle arrest. Molecules 19 (9), 14383–14395.

Qiu, P., Liu, J., Zhao, L., Zhang, P., Wang, W., Shou, D., Ji, J., Li, C., Chai, K., Dong, Y., 2022. Inoscavin A, a pyrone compound isolated from a *Sanghuangporus vaninii* extract, inhibits colon cancer cell growth and induces cell apoptosis via the hedgehog signaling pathway. Phytomedicine 96, 153852.

Sarfraz, A., Rasul, A., Sarfraz, I., Shah, M.A., Hussain, G., Shafiq, N., Masood, M., Adem, Ş., Sarker, S.D., Li, X., 2020. Hispolon: a natural polyphenol and emerging cancer killer by multiple cellular signaling pathways. Environ. Res. 190, 110017.

Wang, Q., Qin, X., Liang, Z., Li, S., Cai, J., Zhu, Z., Liu, G., 2018. HPLC–DAD–ESI–MS2 analysis of phytochemicals from Sichuan red orange peel using ultrasound-assisted extraction. Food Biosci. 25, 15–20.

Wu, C.S., Lin, Z.M., Wang, L.N., Guo, D.X., Wang, S.Q., Liu, Y.Q., Yuan, H.Q., Lou, H.X., 2011. Phenolic compounds with NF-κB inhibitory effects from the fungus *Phellinus baumii*. Bioorg. Med. Chem. Lett. 21 (11), 3261–3267.

Yin, C., Shi, D., Chen, Z., Fan, X., Yao, F., Lu, Q., Gao, H., 2022. Comparative analysis of physicochemical characteristics and in vitro biological activities of polysaccharides from γ-irradiated and nonirradiated *Schizophyllum commune*. Radiat. Phys. Chem. 197, 110177.

Yu, J., Dong, X.D., Jiao, J.S., Yu, S.S., Ji, H.Y., Liu, A.J., Chen, Ye, 2022. The inhibitory effects of selenium nanoparticles modified by fructose-enriched polysaccharide from *Codonopsis pilosula* on HepG2 cells. Ind. Crop. Prod. 176, 114335.

Zan, L.F., Guo, H.Y., Bao, H.Y., Tolgor, Fan, Y.G., 2022. Characterization of Cytotoxicity and Chemical Constituents of Extracts of *Sanghuangporus Baumii* Fruiting Bodies. Mycosystema. http://kns.cnki.net/kcms/detail/11.5180.Q.20220412.1819.016.html (in Chinese).

Zhang, J., Yan, X.P., Li, Y.P., Shao, Y.Y., Ye, T.M., Li, X., Jia, H.B., Jiang, S.M., He, X.L., Sun, X.W., 2021. Comparative study on content of main active components in fruiting body of Sanghuang from different sources and harvest stages. Acta Sericologica Sinica 47, 568–574 (in Chinese).

Zhao, X.J., Guo, P.M., Pang, W.H., Zhang, Y.H., Kilmartin, P.A., 2020. A Rapid UHPLC-QqQ-MS/MS method for the simultaneous qualitation and quantitation of coumarins, furocoumarins, flavonoids, phenolic acids in pummelo fruits. Food Chem. 325, 126835.

Zheng, M.Y., Wang, L., Liu, Z., Zhang, W.J., Gao, P., Lu, S.M., 2022. Extraction and identification of α-glucosidase-inhibitory components from *Phellinus baumii*. Acta Agric. Zhejiangensis 34, 949–958 (in Chinese).

Zheng, Y.T., Zhang, Z.J., Lin, J.R., Lv, Y.H., Lin, L., Du, Z.Y., 2019. Evaluation of whitening effect of *Phellinus igniarius* ethanolic extract. Acta Edulis Fungi. 26, 55–62 (in Chinese).

Zhong, S., Jin, Q., Yu, T., Zhu, J., Li, Y., 2020. *Phellinus gilvus*-derived protocatechualdehyde induces G0/G1 phase arrest and apoptosis in murine B16-F10 cells. Mol. Med. Rep. 21 (3), 1107–1114.

Zhou, L.W., Ghobad-Nejhad, M., Tian, X.M., Wang, Y.F., Wu, F., 2022. Current status of 'Sanghuang' as a group of medicinal mushrooms and their perspective in industry development. Food Rev. Int. 38, 589–607.

Zhou, L.W., Vlasak, J., Decock, C., Assefa, A., Stenlid, J., Abate, D., Wu, S.H., Dai, Y.C., 2016. Global diversity and taxonomy of the Inonotus linteus complex (Hymenochaetales, Basidiomycota): *Sanghuangporus* gen. nov., *Tropicoporus excentrodendri* and *T. guanacastensis* gen. et spp. nov., and 17 new combinations. Fungal Divers. 77, 335–347.